UC Davis
UC Davis Previously Published Works

Title
Inducible nitric oxide synthase (iNOS) regulatory region variation in non-human primates

Permalink
https://escholarship.org/uc/item/77g9g2mr

Authors
Roodgar, Morteza
Ross, Cody T
Kenyon, Nicholas J
et al.

Publication Date
2015-04-01

DOI
10.1016/j.meegid.2015.01.015

Peer reviewed

eScholarship.org Powered by the California Digital Library
University of California

Infection, Genetics and Evolution xxx (2015) xxx–xxx

Contents lists available at ScienceDirect

Infection, Genetics and Evolution

journal homepage: www.elsevier.com/locate/meegid

Inducible nitric oxide synthase (*iNOS*) regulatory region variation in non-human primates

Morteza Roodgar [b,c,d,*], Cody T. Ross [c,d,e], Nicholas J. Kenyon [a], Gretchen Marcelino [c], David Glenn Smith [c,d]

[a] University of California, Davis School of Medicine, Department of Internal Medicine, Division of Pulmonary and Critical Care, United States
[b] Department of Veterinary Medicine, University of California, Davis, United States
[c] Molecular Anthropology Laboratory, University of California, Davis, United States
[d] Department of Anthropology, University of California, Davis, United States
[e] Santa Fe Institute, Santa Fe, NM, United States

ARTICLE INFO

Article history:
Received 15 October 2014
Received in revised form 7 January 2015
Accepted 19 January 2015
Available online xxxx

Keywords:
iNOS
NOS2A
Immune response
Non-human primates
Regulatory region

ABSTRACT

Inducible nitric oxide synthase (*iNOS*) is an enzyme that plays a key role in intracellular immune response against respiratory infections. Since various species of nonhuman primates exhibit different levels of susceptibility to infectious respiratory diseases, and since variation in regulatory regions of genes is thought to play a key role in expression levels of genes, two candidate regulatory regions of *iNOS* were mapped, sequenced, and compared across five species of nonhuman primates: African green monkeys (*Chlorocebus sabaeus*), pig-tailed macaques (*Macaca nemestrina*), cynomolgus macaques (*Macaca fascicularis*), Indian rhesus macaques (*Macaca mulatta*), and Chinese rhesus macaques (*M. mulatta*). In addition, we conducted an *in silico* analysis of the transcription factor binding sites associated with genetic variation in these two candidate regulatory regions across species. We found that only one of the two candidate regions showed strong evidence of involvement in *iNOS* regulation. Specifically, we found evidence of 13 conserved binding site candidates linked to *iNOS* regulation: *AP*-1, *C/EBPB*, *CREB*, *GATA*-1, *GATA*-3, *NF-AT*, *NF-AT*5, *NF-κB*, *KLF*4, *Oct*-1, *PEA*3, *SMAD*3, and *TCF*11. Additionally, we found evidence of interspecies variation in binding sites for several regulatory elements linked to *iNOS* (*GATA*-3, *GATA*-4, *KLF*6, *SRF*, *STAT*-1, *STAT*-3, *OLF*-1 and *HIF*-1) across species, especially in African green monkeys relative to other species. Given the key role of *iNOS* in respiratory immune response, the findings of this study might help guide the direction of future studies aimed to uncover the molecular mechanisms underlying the increased susceptibility of African green monkeys to several viral and bacterial respiratory infections.

© 2015 Elsevier B.V. All rights reserved.

1. Introduction

Inducible nitric oxide synthase (*iNOS*) is an enzyme that plays a key role in immune response against pathogens through the production of peroxinitrite in macrophages (Chan et al., 1992; MacMicking et al., 1997). Genetic changes in the regulatory and/or coding regions of *NOS2A*, the gene encoding *iNOS*, might play an important role in modulating expression levels of *iNOS* and, consequently, cause variation in immune response against intracellular pathogens (Nanashima et al., 2012). Several studies indicate that genetic changes in the regulatory and/or coding region of *NOS2A* are associated with susceptibility to various diseases (Nanashima et al., 2012; Park et al., 2014; Lim et al., 2013; AlFadhli et al., 2013; Fabisiewicz et al., 2013; Karasneh et al., 2011; Wang et al., 2013; Rafiei et al., 2012; Zhang et al., 2011; Planche et al., 2010; Levesque et al., 2010). It has been shown, for example, that mutations in the promoter region of *NOS2A* correlate with susceptibility to malaria (Levesque et al., 2010) and that *iNOS* expression levels are strongly driven by exposure to *Mycobacterium tuberculosis* vaccination (Roodgar et al., 2013). In addition, recent epigenetic studies of the promoter and enhancers of *NOS2A* in humans demonstrate the effect of changes in *NOS2A* regulatory regions on *iNOS* expression (Gross et al., 2014) and the pathogenesis of infectious diseases (de Andrés et al., 2013; Angrisano et al., 2012; Jia et al., 2011; Hobbs et al., 2002).

In this study, we investigated the patterning and functional significance of variation in two candidate regulatory regions of *NOS2A* (which we label *R*1 and *R*2 for notational convenience, see definitions in Section 4) across five taxa of non-human primates (NHPs) relevant to biomedical research: African green monkeys

* Corresponding author at: Department of Veterinary Medicine, University of California, Davis, United States.
E-mail addresses: mroodgar@ucdavis.edu (M. Roodgar), ctross@ucdavis.edu (C.T. Ross).

http://dx.doi.org/10.1016/j.meegid.2015.01.015
1567-1348/© 2015 Elsevier B.V. All rights reserved.

Please cite this article in press as: Roodgar, M., et al. Inducible nitric oxide synthase (*iNOS*) regulatory region variation in non-human primates. Infect. Genet. Evol. (2015), http://dx.doi.org/10.1016/j.meegid.2015.01.015

UNCORRECTED PROOF

(*Chlorocebus sabaeus*), pig-tailed macaques (*Macaca nemestrina*), cynomolgus macaques (*Macaca fascicularis*), Indian rhesus macaques (*M. mulatta*), and Chinese rhesus macaques (*M. mulatta*). Variation in regulation of *iNOS* expression may play a role in the variable susceptibility of these species to several infectious diseases (Roodgar et al., 2013; Lyashchenko et al., 2007; McAuliffe et al., 2004). We investigated whether or not there is evidence for interspecies differences in the regulatory regions of *iNOS* that might account for such variability in disease susceptibility. Since *NOS2A* plays a key role in immunity against intracellular pathogens (Wienerroither et al., 2014; Obermajer et al., 2013) relevant to human health, information on DNA sequence variation in the regulatory region of *NOS2A* in species of NHP that are more closely related to humans than the mouse should provide better information about the relationship between variation in *NOS2A* gene expression and human-like immune responses to intracellular pathogens (Lyashchenko et al., 2007; McAuliffe et al., 2004).

We sequenced two candidate regulatory regions of the *NOS2A* gene in several animals in each of five species or subspecies of NHP that exhibit differing levels of susceptibility to infectious respiratory diseases, especially tuberculosis. The basic primer sequences for the candidate *iNOS* promoter regions were identified using the human genome Chip-seq data available at the University of California, Santa Cruz (UCSC) Genome Browser. We then used an Applied Biosystems 3130XL genetic analyzer to produce DNA sequence data for each sample. Sequences were aligned using Kalign2 (Lassmann et al., 2009; Lassmann and Sonnhammer, 2006; Lassmann and Sonnhammer, 2005), and variation in the candidate promoter regions was analyzed using the *adegenet* package in the R programming environment (R Core Team, 2014). The effect of cross-species genetic conservation and variation on transcription factor and regulatory element bindings sites was then evaluated using the MatInspector software (Quandt et al., 1995; Cartharius et al., 2005).

2. Results

2.1. Multiple sequence alignment and promoter localization

We localized the *iNOS* coding region and the candidate promoter/regulatory regions on the rhesus macaque and human reference sequences using the NCBI genome browser. Fig. 1 plots the location of the *R*2 region on the human reference sequence.

Multiple sequence alignment of *R*1 and *R*2 across species was conducted using Kalign2 (Lassmann et al., 2009; Lassmann and Sonnhammer, 2006; Lassmann and Sonnhammer, 2005). The performance of the alignment was evaluated using Mumsa (Lassmann and Sonnhammer, 2006) and visual inspection. The Jalview program (Clamp et al., 2004; Waterhouse et al., 2009) was used to visualize and trim the alignments and construct species-specific consensus sequences. In Fig. 2, we plot the animal-specific nucleotide sequences and species-specific consensus sequences used in this analysis.

2.2. Promoter variation and interspecies clustering

To investigate whether or not variation in *R*1 and *R*2 followed the pattern expected from the phylogenetic relationships among these NHP species and subspecies, we used the R packages *ape* and *adegent* to extract the SNPs from the aligned and trimmed DNA sequences. We then used discriminant analysis of principal components (DAPC) (Jombart et al., 2010) to investigate the cross-species partitioning of genetic variation.

Fig. 3 plots the location of all animals included in this study on the first two principal components of variation. Fig. 3 illustrates that for both *R*1 and *R*2 the first principal component separates African green monkeys from the other species. The second principal component separates Chinese and Indian rhesus macaques from cynomolgus and pig-tailed macaques. In the *R*1 region, the second principal component fails to separate Chinese rhesus macaques from Indian rhesus macaques and cynomolgus macaques from pig-tailed macaques. In the *R*2 region, the second principal component separates Chinese rhesus macaques from Indian rhesus macaques to some extent, while cynomolgus macaques and pig-tailed macaques remain unseparated.

Fig. 4 illustrates the group assignment probabilities based on the DAPC analysis of SNPs in the *R*1 and *R*2 regions. We find that African green monkeys can be distinguished from other species with high probability at both *R*1 and *R*2. In *R*2, but not *R*1, Indian rhesus, and to some extent Chinese rhesus, can be discriminated from other species with high probability. In both *R*1 and *R*2, cynomolgus macaques cannot be distinguished from pig-tailed macaques.

2.3. In silico regulatory element and transcription factor binding site analysis

To understand the possible phenotypic consequence of genetic variation in the *R*1 and *R*2 regions and identify whether or not each region is likely to be involved in regulation of *iNOS* transcription, we conducted an *in silico* analysis of regulatory element (RE) and transcription factor (TF) binding to the DNA sequences in *R*1 and *R*2 using MatInspector (Quandt et al., 1995; Cartharius et al., 2005). We identified several key RE and TF bindings sites inside both *R*1 and *R*2. Many of these sites were conserved across all species included in this analysis. Notably, region *R*2 contains binding sites for the majority of REs and TFs known from laboratory studies to influence *iNOS* expression (see Section 3), while the *R*1 region lacks binding sites for almost all of these elements.

We also identified several species-specific RE and TF bindings sites, indicating that variation in TF and RE binding to the DNA sequences of *R*1 and *R*2 is influenced by the SNPs discovered in this analysis. We detail these findings in the subsections that follow.

2.3.1. Cross species conservation

We found 39 RE/TF binding sites that were conserved across all animals in *R*1 and 71 that were conserved across all animals in *R*2. Supplementary Table 1 contains the full list of the MatInspector Matrix IDs of these REs and TFs. Notably, in *R*2 , binding sites for *AP*-1, *C/EBPB*, *CREB*, *GATA*-1, *GATA*-3, *NF-AT*, *NF-AT*5, *NF-κB*, *KLF*4, *Oct*-1, *PEA*3, *SMAD*3, and *TCF*11, 13 genes that have been previously associated with *iNOS* regulation (Pautz et al., 2010; Liao et al., 2011), were conserved. In contrast, only 2 binding sites previously associated with *iNOS* regulation were conserved in *R*1 (*PPAR-γ* and *USF*-1) (Pautz et al., 2010).

2.3.2. Cross species variation

We identified 105 RE/TF binding sites in *R*1 and 95 RE/TF binding sites in *R*2 which included a SNP that disrupted the simulated binding of the REs and TFs to the DNA sequence. Supplementary Table 2 contains the full list of the MatInspector Matrix IDs of these REs and TFs, paired with annotations and the animal specific data. To identify which of these binding sites were predictive of interspecies differences, we used an ℓ_1-regularized categorical Bayesian multiple regression model to classify animals into three groups (African green monkeys, Chinese/Indian rhesus macaque, or cynomolgus/pig-tailed macaque), using the existence or non-existence of RE and TF bindings sites as predictors. The maximum *a posteriori* parameter vector representing the strength of association between any RE or TF binding site and all three outcome categories can be plotted in barycentric space using a tertiary plot to represent the

UNCORRECTED PROOF

Please cite this article in press as: Roodgar, M., et al. Inducible nitric oxide synthase (*iNOS*) regulatory region variation in non-human primates. Infect. Genet. Evol. (2015), http://dx.doi.org/10.1016/j.meegid.2015.01.015

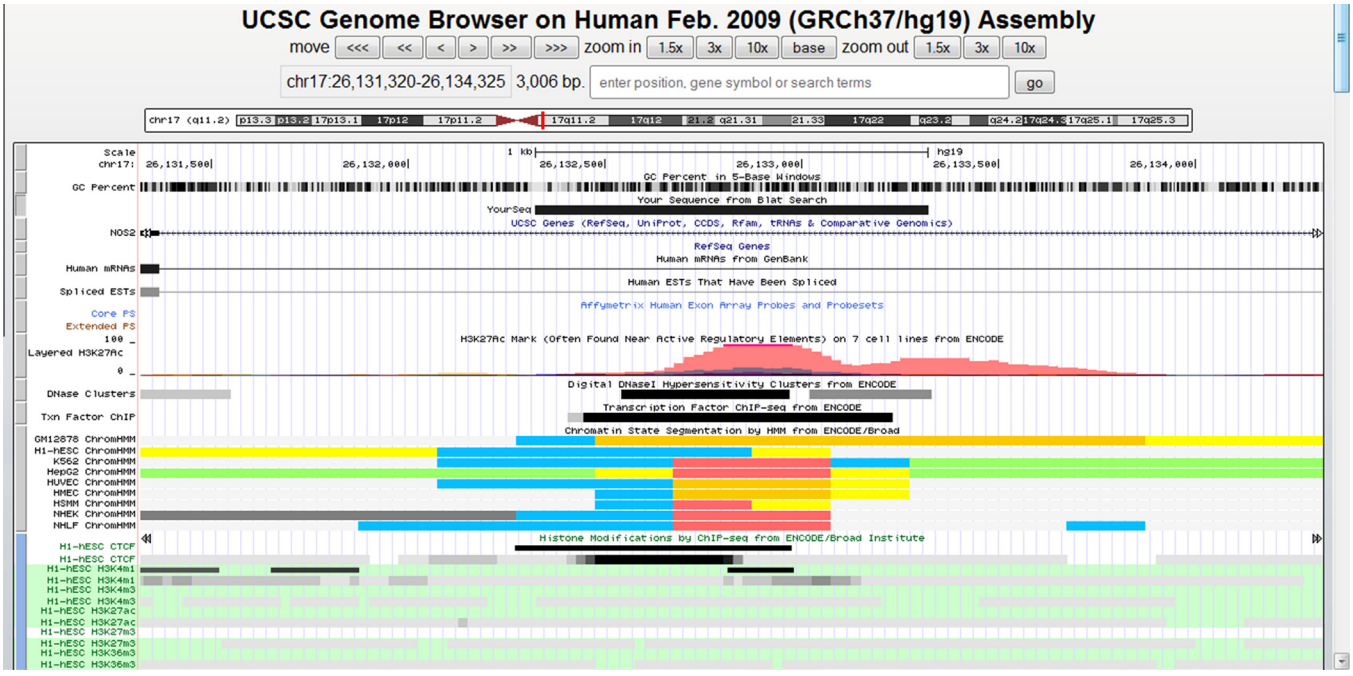

Fig. 1. Location of the *iNOS* coding region and the *R*2 candidate promoter/regulatory region on the human reference frame.

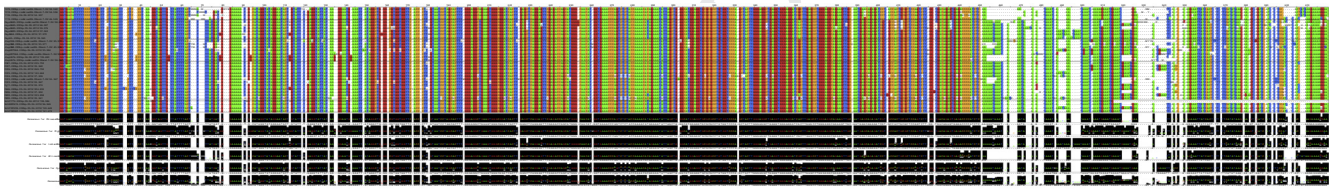

(a) Alignment and Consensus sequences of *R*1

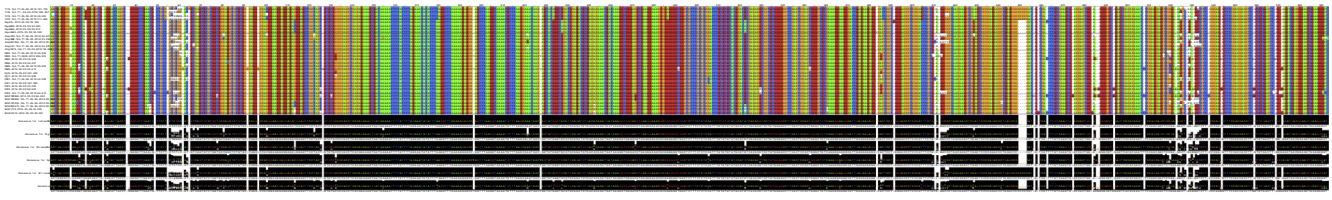

(b) Alignment and Consensus sequences of *R*2

Fig. 2. Results of multiple sequence alignment in regions *R*1 (Frame 2a) and *R*2 (Frame 2b).

relative strength of association across categories. Fig. 5 displays such plots for *R*1 and *R*2 . Each colored letter represents an RE or TF binding site and links it to its gene name in Supplementary Table 3.

Most points in the tertiary plot are shrunken towards the center of the plotting space by the regularizing priors of the Bayesian model, showing that most variation in binding sites is not indicative of cross species differences. However, a few RE/TF binding sites in both *R*1 and *R*2 reflect differences between African green monkeys and the other species. For example, in *R*1, binding sites for *GATA*-3, *MEIS*1, *PU*.1/*SPI*-1, and *EBF*1 show increased association with African green monkeys, and those for *HOXB*8, *GATA*-4, *DLX*3, *CDX*1, *HOXA*9, *HOXB*6, *IRF*4, *ZNF*384, *TEF*, *NF-AT*5, *MSX*3, *MEOX*1, and *HSF*2 show a decreased association with African green monkeys, relative to other species.

In *R*2 we find an increased association of binding sites for *GCM*1, *GLIS*2, *KLF*6, *MAZ*, *MTBF*, *NM*23, *PAX*6, *RTR*, *SRF*, *STAT*-1, *STAT*-3, *ZIC*2, and *ZNF*219 with African green monkeys, and a decreased association of *ELF*-1, *GLS*3, *HOXB*9, *SMARCA*2, *OLF*-1, and *TIEG* with African green monkeys, relative to other species.

It is also notable that binding sites for *PAX*3 and *HIF*-1 are negatively associated with rhesus macaques relative to the other groups.

3. Discussion

3.1. Promoter variation and interspecies clustering

The results of this study indicate that genetic divergence in *R*1 and *R*2 across species roughly corresponds to that which would be

Please cite this article in press as: Roodgar, M., et al. Inducible nitric oxide synthase (*iNOS*) regulatory region variation in non-human primates. Infect. Genet. Evol. (2015), http://dx.doi.org/10.1016/j.meegid.2015.01.015

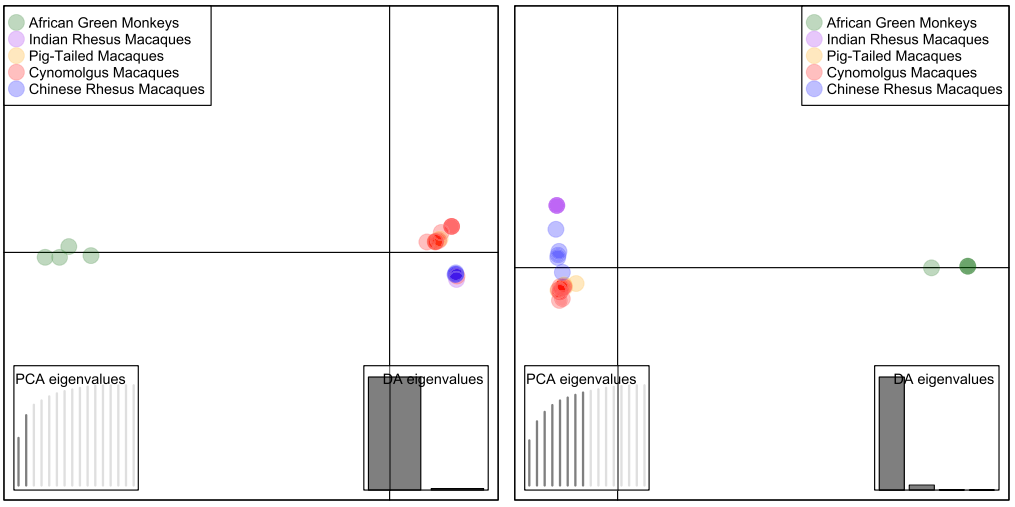

(a) Scatterplot of animals in the first two principal components, *R*1.

(b) Scatterplot of animals in the first two principal components, *R*2.

Fig. 3. Discriminant analysis of principal components in regions *R*1 (Frame 3a) and *R*2 (Frame 3b). The first principal component (horizontal axis) separates African green monkeys from the other species in both *R*1 and *R*2. The second principal component (vertical axis) separates Rhesus macaques from cynomolgus and pig-tailed macaques.

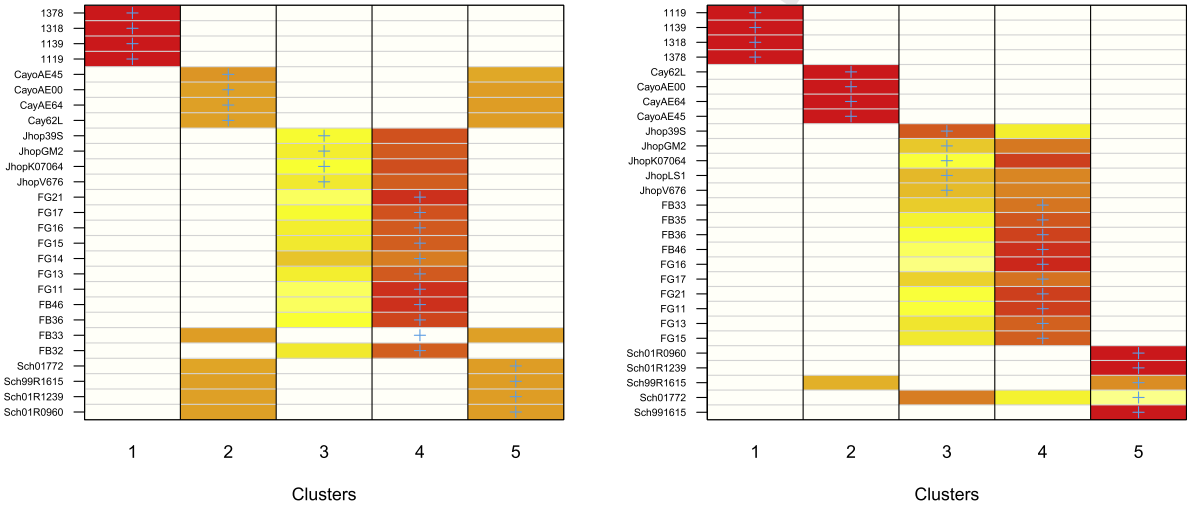

(a) Group assignment probability plot of animals using region *R*1.

(b) Group assignment probability plot of animals using region *R*2.

Fig. 4. Group assignment plots based on DAPC analysis of regions *R*1 (Frame 4a) and *R*2 (Frame 4b). The row labels are animal IDs (the numeric values are African green monkeys, the *Cay* prefix indicates Indian rhesus macaques, the *Jhop* prefix indicates pig-tailed macaques, the *FG* and *FB* prefixes are cynomolgus macaques, and the *Sch* prefix indicates Chinese rhesus macaques). The blue crosses indicate the true group assignment, and the cell color indicates increasing group assignment probability (based on SNP data) as the scale shifts from yellow to red. We note three distinct genetic clusters in *R*1 (African green monkey, rhesus macaque, and cynomolgus/pig-tailed macaques), and four distinct genetic clusters in *R*2 (African green monkey, Indian rhesus macaque, Chinese rhesus macaque, and cynomolgus/pig-tailed macaques). (For interpretation of the references to color in this figure legend, the reader is referred to the web version of this article.)

expected from phylogenetic relationships. African green monkeys exhibit the most distant evolutionary relationship with the other species, followed in order by pig-tailed macaques, cynomolgus macaques, Chinese rhesus macaques (with gene flow to cynomolgus macaques), and finally Indian rhesus macaques, the most highly derived of the five taxa (Hayasaka et al., 1996). However, in contrast to expectations under purely neutral evolution, pig-tailed and cynomolgus macaques exhibit greater clustering than cynomolgus and Chinese rhesus macaques even though the evolutionary distance between pig-tailed and cynomolgus macaques is greater than that between cynomolgus and Chinese rhesus macaques (Tosi et al., 2000). This pattern of divergence of rhesus from other species might be indicative of rhesus specific selection or demographic effects.

3.2. In silico regulatory element and transcription factor binding site analysis

3.2.1. Conserved RE/TF binding sites

In this study, we discovered 13 conserved binding site candidates linked to *iNOS* regulation (*AP*-1, *C/EBPB*, *CREB*, *GATA-1*,

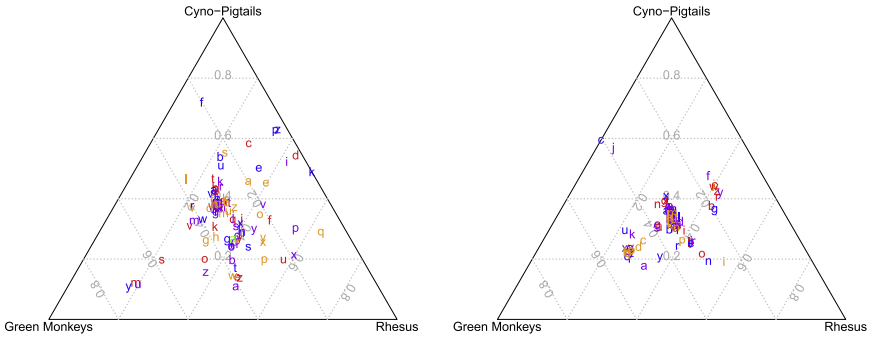

(a) RE and TF binding sites and species classification in *R*1

(b) RE and TF binding sites and species classification in *R*2

Fig. 5. The associations between RE and TF binding sites and species classification in regions *R*1 (Frame 5a) and *R*2 (Frame 5b). Each colored letter represents an RE/TF binding site (see Supplementary Materials Table 3 for the codebook linking each RE/TF binding site to each data point in the plot) plotted in barycentric space using a tertiary plot to represent the relative strength of association across categories. Data points in the center cluster of the plotting space are not indicative of interspecies differences in RE/TF binding sites; data points located near the boundary of the triangle are indicative of interspecies differences in RE/TF binding. Only a small fraction of the RE/TF binding sites identified in our analysis are indicative of interspecies differences.

GATA-3, NF-AT, NF-AT5, NF-κB, KLF4, Oct-1, PEA3, SMAD3, and TCF11) in R2 across species. In addition to the results of in silico analyses presented here (Pautz et al., 2010; Liao et al., 2011; Kleinert et al., 2004), many of these transcription factors have been shown to play a key role in the regulation of *iNOS* expression in laboratory studies. In contrast, we identified only two conserved binding sites previously linked to *iNOS* regulation (*PPAR-γ* and *USF*-1) in *R*1 (Pautz et al., 2010). These results provide evidence that *R*2 is a more appropriate candidate region for *iNOS* regulation in these species of NHPs than *R*1.

In the list of conserved RE/TF binding sites across these species of NHP, *NF-κB* is the most well-studied transcription factor known an important role in regulation of *iNOS* expression (Uffort et al., 2009; Chan et al., 2001; Jaramillo et al., 2003; Oussaief et al., 2011; Kelleher et al., 2007; Feng et al., 2002). Previous studies have shown that *NF-κB* modulates *iNOS* expression during various viral, bacterial, and parasitic infections (Oussaief et al., 2011; Chan et al., 2001; Jaramillo et al., 2003). It has also been shown that interference in the *NF-κB*-dependent regulation of *iNOS* expression is part of the pathogenic mechanism for *Helicobacter pylori* (Kim et al., 2003); a similar mechanism may be involved in the pathogenesis of other infectious diseases (e.g., *Mycobacterium tuberculosis).*

3.2.2. Non-conserved RE/TF binding sites

While searching for interspecies differences in TF binding sites in *R*1 and *R*2, we found evidence of a decreased association of binding sites for *HOXB*8, *GATA*-4, *DLX*3, *CDX*1, *HOXA*9, *HOXB*6, *IRF*4, *ZNF*384, *TEF*, *MSX*3, *MEOX*1, and *HSF*2 with African green monkeys relative to other species in *R*1, as well as a decreased association of binding sites for *ELF*-1, *GLS*3, *HOXB*9, *SMARCA*2, *OLF*-1, and *TIEG* with African green monkeys relative to other species in *R*2.

Additionally, we found an increased association of binding sites for *GATA*-3, *MEIS*1, *PU*.1/*SPI* – 1, and *EBF*1 in *R*1, and an increased association of binding sites for *GCM*1, *GLIS*2, *KLF*6, *MAZ*, *MTBF*, *NM*23, *PAX*6, *RTR*, *SRF*, *STAT*-1, *STAT*-3, *ZIC*2, and *ZNF*219 in *R*2, with African green monkeys relative to other species.

Some of the SNPs we have identified might be responsible for interspecies differences in *iNOS* regulation and expression, as well as susceptibility to diseases linked to *iNOS* expression levels, such as tuberculosis. While there is no clear biological link between many of the genes cited above and *iNOS* production, several of these genes (e.g. *GATA*-3, *GATA*-4, *KLF*6, *SRF*, *STAT*-1, *STAT*-3, *OLF*-1 and *HIF*-1) have been linked to *iNOS* regulation in laboratory studies (Pautz et al., 2010).

3.3. Candidate genes for interspecies differences in iNOS regulation

3.3.1. STAT

Given the significant role of *STAT* proteins in inducing IFN-dependent expression of MHC II in macrophages (Zhao et al., 2007), interspecies variation in *STAT* binding sites might contribute to variation in innate immune response across these species. *STAT*-1, specifically, is known to be an important transcription factor for regulating *iNOS* expression (Ganster et al., 2001; Ohmori and Hamilton, 2001). Since several studies indicate a significant role for *STAT*-1 in *iNOS* activation and expression (Samardzic et al., 2001), variation in *STAT*-1 binding sites across these species might contribute to variable susceptibility to respiratory diseases, given the role of *iNOS* expression in immune response to respiratory infection (Roodgar et al., 2013). Moreover, *STAT*-1 plays a key role in inducing the expression of IFN-inducible 10kD protein (*IP*-10) and interferon regulatory factor 1 (*IRF*-1), which are also known to play key roles in innate immune response by macrophages (Ohmori and Hamilton, 2001). Future *in vivo* investigations may clarify the influence of genetic changes in *STAT*-1 binding sites in *iNOS* regulatory regions across non-human primates on susceptibility to respiratory diseases.

3.3.2. KLF

Among these species of NHP, African green monkeys, but not members of the other species, exhibit a binding site for kruppel-like factor 6 (*KLF*6), a key transcription factor of *iNOS*. Several studies indicate that *KLF*6, which transactivates *iNOS* expression (Warke et al., 2003), plays a key role in immunity against viral and bacterial respiratory infections. A direct interaction between *KLF*6 and *iNOS* has been observed in *in vitro* infection of human lung cells with influenza A virus (Mgbemena et al., 2012). *KLF*6 also regulates apoptosis through the activation of *iNOS* expression and plays a critical role in *iNOS* expression during respiratory syncytial virus (RSV) (Mgbemena et al., 2013) and influenza A virus infection (Mgbemena et al., 2012).

3.4. Binding site differences in African green monkeys

The African green monkey has been widely used as an animal model for viral and bacterial respiratory diseases (e.g., RSV and *M. tuberculosis* (MTB) (Bukreyev et al., 2004; Tang et al., 2004; Jin et al., 2003; Lyashchenko et al., 2007) to which rhesus and cynomolgus macaques seem less susceptible. For example, African

UNCORRECTED PRC

green monkeys exhibit more severe symptoms when infected with MTB (Lyashchenko et al., 2007). Previous studies also indicate that replication of SARS virus occurs more rapidly in African green monkeys than in cynomolgus and rhesus macaques (McAuliffe et al., 2004).

Because of the key role of *iNOS* in innate immune response against respiratory disease pathogens and the unique presence of binding sites for *STAT*-1, *KLF*6, and other *iNOS* REs/TFs in African green monkeys relative to the other considered species, these RE/TF binding sites may play a role in the varying levels of susceptibility to viral and bacterial respiratory infections across these NHP species. However, variation in susceptibility to respiratory diseases is clearly multifactorial and regulated by many genes. Variation in binding sites for the above REs/TFs (i.e., *STAT*-1 and *KLF*6), however, might partially explain variation in *iNOS* expression, and subsequently variation in innate immune response to respiratory infections.

More detailed laboratory studies are required to investigate: (1) if the RE/TF binding sites discovered through our *in silico* analysis are actually representative of biologically-relevant, *in vivo*, binding sites, (2) how these binding sites, if biologically relevant, modulate *iNOS* expression across species of NHP, and (3) how variation in *iNOS* expression is related to variation in disease susceptibility across species.

4. Materials and methods

4.1. Study subjects, sample preparation, and DNA extraction

DNA was extracted from lung tissue of 12 cynomolgus macaques (*M. fascicularis*) from the Tulane National Primate Research Center that were previously used in a tuberculosis study (Roodgar et al., 2013), and from blood drawn from 5 Indian and 5 Chinese rhesus macaques (*M. mulatta*) from the California National Primate Research Center, 5 pig-tailed macaques (*M. nemestrina*) from Johns Hopkins University, and 6 African green monkeys (*C. sabaeus*) from the Wake Forest Primate Center using Qiagen QIAamp DNA Mini Kit (Qiagen Inc., Valencia, CA) following the manufacturer's protocol.

4.2. Candidate promoter regions of iNOS

The first candidate regulatory region for *iNOS* that we label *R*1, for convenience, had been previously described in the literature (*see* Nunokawa et al., 1994).

A second candidate regulatory region for *iNOS* that we label *R*2 was mapped using the UCSC genome browser. The *R*2 region lays approximately 700–1000 bp upstream of the first exon of *iNOS* and was identified as a regulatory region candidate through visual inspection of the UCSC genome browser (*see* Fig. 1) and literature review (*see* Pautz et al., 2010). This region corresponds to the peak of *H3K4me3* in normal lung fibroblasts, and according to the UCSC genome browser, contains several transcription factor binding sites (TFBS). The location of the orthologous sequence in NHP species was located using the UCSC genome browser and the Basic Local Alignment Tool (BLAT).

4.2.1. Primer design and sequencing of two possible regulatory regions of iNOS

Two sets of primers were designed and tested to amplify the *R*1 candidate regulatory region for *iNOS* (Nunokawa et al., 1994). Primer set 1 was composed of forward and reverse primers 5′*GGCAA TGAGTGGACACTGGCA*3′ and 5′*TGGCACAGAGATGCCTCTGAGAAGT*3′, respectively, and primer set 2 was composed of forward and reverse primers 5′*GGAAGGCAATGAGTGGACACTGGC*3′ and 5′*GCTTTG GCAGAATGGCAAGTAGGA*3′, respectively.

Two sets of primers were used to amplify the *R*2 region: primer set 1 was composed of forward and reverse primers 5′*CTACAGGTG AGTACACCCAGGAGCA*3′ and 5′*GGCCTGTCCACCCTGGAGTGA*3′, respectively, and primer set 2 was composed of forward and reverse primers 5′*CCCAGGAGCAAGGAGAGGTGACA*3′ and 5′*TGACTCACGCCC TCCAGTGGT*3′, respectively.

The primers described above were tested using a gradient to optimize the annealing temperature for the polymerase chain reaction (PCR). The PCR conditions used to amplify these two candidate regions for 60 PCR cycles were: an initial hold at 94 °C for 3 min, followed by denaturing at 94 °C for 30 s, annealing at either 58.7 °C for 20 s (for *R*2) or 57.4 °C for 20 s (for *R*1), extension at 72 °C for 45 s, and a final hold at 72 °C for 5 min.

The amplified products were first quantified and checked by agarose and native acrylamide gel electrophoresis. DNA sequencing was accomplished using the ABI BigDye Terminator sequencing chemistry and an ABI 3130XL DNA sequencer (Applied Biosystems, Inc., Foster City, CA, USA) at the Molecular Anthropology Laboratory (MAL) at UC Davis.

4.3. Multiple sequence alignment

Multiple sequence alignment was conducted with the command line version of Kalign2 (Lassmann et al., 2009; Lassmann and Sonnhammer, 2006, 2005) using several hundred parameter permutations. The command line version of Mumsa (Lassmann and Sonnhammer, 2006) was used to select the best performing alignments. The best performing alignments were then visually inspected and the procedure was repeated until a sequence alignment with no noticeable pathologies was obtained.

The parameters used to obtain the final alignments for *R*1 were: gap open penalty = 10, gap extension penalty = 1, and terminal gap penalty = 3. For *R*2 , the final alignment parameters were: gap open penalty = 40, gap extension penalty = 1, and terminal gap penalty = 6.

The Jalview program (Clamp et al., 2004; Waterhouse et al., 2009) was used to visualize the sequence alignments and obtain consensus sequences.

4.4. SNP identification and statistical analysis

The R Environment for Statistical Computing (R Core Team, 2014) was used for all SNP-based analysis of aligned sequences and visualization of the results from the simulated regulatory element and transcription factor binding analysis.

4.4.1. SNP identification

SNPs were extracted from the aligned sequences using the *ape* (Paradis et al., 2004) and *adegenet* (Jombart, 2008) packages in R. Twenty-eight SNPs were identified in the trimmed version of *R*1 (at locations 4,7, 36, 68, 120, 135, 206, 288, 362, 394, 403, 406, 467, 478, 488, 492, 501, 509, 543, 550, 580, 592, 598, 599, 606, 612, 617, and 619 of the sequence). Twenty-eight SNPs were also identified in the trimmed version of *R*2 (at locations 13, 19, 54, 81, 83, 101, 114, 123, 133, 155, 180, 222, 234, 238, 272, 287, 306, 323, 367, 386, 387, 405, 429, 485, 520, 591, 592, and 593 of the sequence). Tables 1 and 2 plot the sample frequencies of each SNP by species.

4.4.2. Discriminant analysis of principal components

The *adegenet* (Jombart, 2008) package was utilized to conduct discriminant analysis of principal components (Jombart et al., 2010) of the SNP data for each of the two sequence alignments.

UNCORRECTED PROOF

Table 1
Sample SNP frequencies by species in region *R*1.

SNP location	African green monkey	Indian rhesus macaque	Pig-tailed macaque	Cynomolgus macaque	Chinese rhesus macaque
4	0	0	0	0.083	0
7	0	1	1	1	1
36	0	1	1	1	1
68	0.333	1	1	1	1
120	0	0	0.143	0	0
135	NA	NA	0.667	NA	NA
206	0	1	1	1	1
288	0	1	0	0.083	1
362	0	1	0	0.083	1
394	0.5	1	1	1	1
403	0	1	1	1	1
406	0	1	1	1	1
467	NA	0	1	NA	NA
478	0	0	0.143	0	0
488	1	1	0.857	1	1
492	NA	1	0	1	1
501	1	1	0.715	1	1
509	1	0	0	0	0
543	0.75	1	1	1	1
550	1	0.75	1	1	1
580	1	1	1	0.917	1
592	1	0.667	1	1	1
598	1	1	0.857	1	1
599	1	1	0.857	1	1
606	0.75	1	1	0.667	1
612	1	0.833	1	1	1
617	0.75	1	1	1	1
619	1	1	0.857	1	1

Table 2
Sample SNP frequencies by species in region *R*2.

SNP location	African green monkey	Indian rhesus macaque	Pig-tailed macaque	Cynomolgus macaque	Chinese rhesus macaque
13	0	0	0	0	0.167
19	0	0	0	0.077	0
54	0	1	1	1	1
81	0	0	0.25	0	0
83	0	0	0	0.077	0
101	0	1	1	1	1
114	0	1	0	0	0.5
123	0	0	0.25	0	0
133	0	0	0	0.25	0
155	0	0	0.2	0	0
180	0	1	1	1	1
222	0	0	0.333	0	0
234	0	1	1	1	1
238	0	1	0	0	0
272	0	0	0	0	0.333
287	0	1	1	1	1
306	0	0	0	0.154	0
323	0	1	0	0	0.4
367	0	0	0	0.077	0
386	0	0	0	0.5	0
387	0	1	1	1	1
405	0	1	1	1	1
429	0	1	1	1	1
485	0	0	0	0.154	0.2
520	0	0	0	0.667	0
591	0	0	0.2	0.077	0
592	0	0	0	0.077	0
593	0	0	0.2	0	0

UNCORRECTED PROOF

Further, *adegenet* was used to produce visualizations of these results both as scatter plots and group assignment probability plots.

4.4.3. Simulated transcription factor binding analysis

We used the MatInspector software (Quandt et al., 1995; Cartharius et al., 2005) to search for RE and TF binding sites located inside *R*1 and *R*2. This analysis used the most conservative default parameters settings in MatInspector and was conducted independently on each animal's aligned and trimmed FASTA formatted sequence.

MatInspector returns a large list of possible RE/TF binding sites for each DNA sequence. Because we are interested in understanding both conservation of and variation in RE/TF binding in *R*1 and *R*2 across species, we divided the full list of candidate RE/TF binding sites into two smaller list: (1) a list of RE/TF binding sites that

Please cite this article in press as: Roodgar, M., et al. Inducible nitric oxide synthase (*iNOS*) regulatory region variation in non-human primates. Infect. Genet. Evol. (2015), http://dx.doi.org/10.1016/j.meegid.2015.01.015

did not include SNPs and were, therefore, conserved across species, and (2) a list of RE/TF binding sites that included at least one of the 28 SNPs and were, therefore, variable across animals/species.

4.4.4. An ℓ_1-regularized categorical bayesian multiple regression model

For each region, *R*1 and *R*2, we investigated how variation in RE/TF binding sites was associated with the classification of animals into the $K = 3$ major clusters observed in our data: African green monkeys, Chinese and Indian rhesus macaques, and cynomolgus and pig-tailed macaques. We used a categorical regression model to predict the classification, $Y_{[n]} \in \{1 \ldots K\}$, of animal n using data on the RE/TF binding profile of that animal. Each RE/TF binding profile, $X_{[1\ldots(P+1),n]}$, is a vector beginning with an intercept value of 1, and continuing with $P = 105$ (in *R*1, or $P = 95$ in *R*2) binary data points that indicate the presence or absence of the p_{th} RE/TF binding site in animal n. Because we had many more predictors than animals in our sample, we used a full Bayesian regression model with Laplace (also known as double exponential) priors on the regression coefficients. This model formulation imposes the Bayesian corollary of Lasso, or ℓ_1-regularized regression, which penalizes the number of non-zero parameter values, reducing effective model complexity (Tibshirani, 1996). Accordingly, each outcome is modeled as:

$$Y_{[n]} \sim \text{Categorical } (\phi_{[n]}) \tag{1}$$

where:

$$\phi_{[n]} = \text{Softmax } (\beta * X_{[1\ldots(P+1),n]}) \tag{2}$$

and β is a K by $P+1$ matrix of parameters representing the intercepts as well as the associations of each of the P predictors with each of the K outcome categories. The Softmax function is defined for a K-vector $\theta \in \mathbb{R}^K$ as:

$$\text{Softmax } (\theta) = \left(\frac{e^{\theta_{[1]}}}{\sum_{k=1}^{K} e^{\theta_{[k]}}}, \ldots, \frac{e^{\theta_{[K]}}}{\sum_{k=1}^{K} e^{\theta_{[k]}}} \right) \tag{3}$$

and yields a vector in the unit K-simplex which is appropriate to use as the parameter vector for a categorical distribution. The Softmax function is invariant under adding a constant to each component of its input (Stan Development Team, 2014), but strongly regularizing priors identify the model.

We declare weakly regularizing Gaussian priors on the intercept parameter for each category where $k \in \{1 \ldots K\}$:

$$\beta_{[k,1]} \sim \text{Normal } (0, 10) \tag{4}$$

and strongly regularizing Laplace priors on the remaining (slope) parameters of the β matrix. Thus, for $k \in \{1 \ldots K\}$ and $p \in \{2 \ldots (P+1)\}$, we model:

$$\beta_{[k,p]} \sim \text{Double Exponential } (0, 0.1) \tag{5}$$

We use Hamiltonian Markov Chain Monte Carlo simulation (Hoffman and Gelman, xxxx) to fit this model. Our Markov chains are coded in templated C++ using the R implementation of the Stan 2.2.0 C++ library (Stan Development Team, 2013). We then use the *vcd* package (Meyer et al., 2006) in R to plot the posterior mean estimate of each $\beta_{[1\ldots K,p]}$ parameter vector in barycentric coordinates. Points located in the center of the barycentric space indicate variables that are not informative about inter-group differences in RE/TF binding sites, while points located near the edges of the barycentric space are indicative of inter-group differences in RE/TF binding sites.

Acknowledgments

The authors gratefully acknowledge the help of Frederic Chedin (Department of Molecular and Cellular Biology UC Davis Genome Center), Satya Dandekar (Medical Microbiology and Immunology School of Medicine, UC Davis, and Linda Lowenstine (Department of Pathology, Microbiology and Immunology, School of Veterinary Medicine UC Davis).

This work was supported by National Institute of Health Grants R24RR05090, R24RR025871, TR000002, and HL105573.

Appendix A. Supplementary data

Supplementary Tables 1, 2, and 3, as well as FASTA formatted sequences for each animal are available online. Supplementary data associated with this article can be found, in the online version, at http://dx.doi.org/10.1016/j.meegid.2015.01.015.

References

AlFadhli, S., Mohammed, E.M., Al Shubaili, A., 2013. Association analysis of nitric oxide synthases: Nos1, nos2a and nos3 genes, with multiple sclerosis. Ann. Hum. Biol. 40 (4), 368–375.

Angrisano, T., Lembo, F., Peluso, S., Keller, S., Chiariotti, L., Pero, R., 2012. *Helicobacter pylori* regulates inos promoter by histone modifications in human gastric epithelial cells. Med. Microbiol. Immunol. 201 (3), 249–257.

Bukreyev, A., Lamirande, E.W., Buchholz, U.J., Vogel, L.N., Elkins, W.R., Claire, M.S., Murphy, B.R., Subbarao, K., Collins, P.L., 2004. Mucosal immunisation of african green monkeys (< i> cercopithecus aethiops)</i> with an attenuated parainfluenza virus expressing the sars coronavirus spike protein for the prevention of sars. The Lancet 363 (9427), 2122–2127.

Cartharius, K., Frech, K., Grote, K., Klocke, B., Haltmeier, M., Klingenhoff, A., Frisch, M., Bayerlein, M., Werner, T., 2005. Matinspector and beyond: promoter analysis based on transcription factor binding sites. Bioinformatics 21 (13), 2933–2942.

Chan, J., Xing, Y., Magliozzo, R., Bloom, B., 1992. Killing of virulent mycobacterium tuberculosis by reactive nitrogen intermediates produced by activated murine macrophages. J. Exp. Med. 175 (4), 1111–1122.

Chan, E.D., Morris, K.R., Belisle, J.T., Hill, P., Remigio, L.K., Brennan, P.J., Riches, D.W., 2001. Induction of inducible nitric oxide synthase-no· by lipoarabinomannan of *Mycobacterium tuberculosis* is mediated by mek1-erk, mkk7-jnk, and nf-κb signaling pathways. Infect. Immun. 69 (4).

Clamp, M., Cuff, J., Searle, S.M., Barton, G.J., 2004. The jalview java alignment editor. Bioinformatics 20 (3), 426–427.

de Andrés, M.C., Imagawa, K., Hashimoto, K., Gonzalez, A., Roach, H.I., Goldring, M.B., Oreffo, R.O., 2013. Loss of methylation in cpg sites in the nf-κb enhancer elements of inducible nitric oxide synthase is responsible for gene induction in human articular chondrocytes. Arthritis Rheum. 65 (3), 732–742.

Fabisiewicz, A., Pacholewicz, K., Paszkiewicz-Kozik, E., Walewski, J., Siedlecki, J.A., 2013. Polymorphisms of dna repair and oxidative stress genes in b-cell lymphoma patients. Biomed. Rep. 1 (1), 151–155.

Feng, X., Guo, Z., Nourbakhsh, M., Hauser, H., Ganster, R., Shao, L., Geller, D.A., 2002. Identification of a negative response element in the human inducible nitric-oxide synthase (hinos) promoter: the role of nf-κb-repressing factor (nrf) in basal repression of the hinos gene. Proc. Natl. Acad. Sci. 99 (22), 14212–14217.

Ganster, R.W., Taylor, B.S., Shao, L., Geller, D.A., 2001. Complex regulation of human inducible nitric oxide synthase gene transcription by stat 1 and nf-κb. Proc. Natl. Acad. Sci. 98 (15), 8638–8643.

Gross, T.J., Kremens, K., Powers, L.S., Brink, B., Knutson, T., Domann, F.E., Philibert, R.A., Milhem, M.M., Monick, M.M., 2014. Epigenetic silencing of the human nos2 gene: rethinking the role of nitric oxide in human macrophage inflammatory responses. J. Immunol., 1301758

Hayasaka, K., Fujii, K., Horai, S., 1996. Molecular phylogeny of macaques: implications of nucleotide sequences from an 896-base pair region of mitochondrial dna. Mol. Biol. Evol. 13 (7), 1044–1053.

Hobbs, M.R., Udhayakumar, V., Levesque, M.C., Booth, J., Roberts, J.M., Tkachuk, A.N., Pole, A., Coon, H., Kariuki, S., Nahlen, B.L., et al., 2002. A new< i> nos2</i> promoter polymorphism associated with increased nitric oxide production and protection from severe malaria in tanzanian and kenyan children. The Lancet 360 (9344), 1468–1475.

M.D. Hoffman, A. Gelman.

Jaramillo, M., Gowda, D.C., Radzioch, D., Olivier, M., 2003. Hemozoin increases ifn-γ-inducible macrophage nitric oxide generation through extracellular signal-regulated kinase-and nf-κb-dependent pathways. J. Immunol. 171 (8), 4243–4253.

Jia, S., Ni, J., Chen, S., Jiang, Y., Dong, W., Gao, Y., 2011. Association of the pentanucleotide repeat polymorphism in nos2 promoter region with susceptibility to migraine in a chinese population. DNA Cell Biol. 30 (2), 117–122.

UNCORRECTED PROOF

Jin, H., Cheng, X., Traina-Dorge, V.L., Park, H.J., Zhou, H., Soike, K., Kemble, G., 2003. Evaluation of recombinant respiratory syncytial virus gene deletion mutants in african green monkeys for their potential as live attenuated vaccine candidates. Vaccine 21 (25), 3647–3652.

Jombart, T., 2008. *adegenet*: a r package for the multivariate analysis of genetic markers. Bioinformatics 24 (11), 1403–1405.

Jombart, T., Devillard, S., Balloux, F., 2010. Discriminant analysis of principal components: a new method for the analysis of genetically structured populations. BMC Genet. 11 (1), 94.

Karasneh, J.A., Darwazeh, A.M., Hassan, A.F., Thornhill, M., 2011. Association between recurrent aphthous stomatitis and inheritance of a single-nucleotide polymorphism of the nos2 gene encoding inducible nitric oxide synthase. J. Oral Pathol. Med. 40 (9), 715–720.

Kelleher, Z.T., Matsumoto, A., Stamler, J.S., Marshall, H.E., 2007. Nos2 regulation of nf-κb by s-nitrosylation of p65. J. Biol. Chem. 282 (42), 30667–30672.

Kim, J.M., Kim, J.S., Jung, H.C., Oh, Y.-K., Chung, H.-Y., Lee, C.-H., Song, I.S., 2003. *Helicobacter pylori* infection activates nf-κb signaling pathway to induce inos and protect human gastric epithelial cells from apoptosis. Am. J. Physiol. Gastrointest. Liver Physiol. 285 (6), G1171–G1180.

Kleinert, H., Pautz, A., Linker, K., Schwarz, P.M., 2004. Regulation of the expression of inducible nitric oxide synthase. Eur. J. Pharmacol. 500 (1), 255–266.

Lassmann, T., Sonnhammer, E.L., 2005. Kalign – an accurate and fast multiple sequence alignment algorithm. BMC Bioinform. 6 (1), 298.

Lassmann, T., Sonnhammer, E.L., 2006. Kalign, kalignvu and mumsa: web servers for multiple sequence alignment. Nucleic Acids Res. 34 (Suppl. 2), W596–W599.

Lassmann, T., Frings, O., Sonnhammer, E.L., 2009. Kalign2: high-performance multiple alignment of protein and nucleotide sequences allowing external features. Nucleic Acids Res. 37 (3), 858–865.

Levesque, M.C., Hobbs, M.R., OLoughlin, C.W., Chancellor, J.A., Chen, Y., Tkachuk, A.N., Booth, J., Patch, K.B., Allgood, S., Pole, A.R., et al., 2010. Malaria severity and human nitric oxide synthase type 2 (nos2) promoter haplotypes. Hum. Genet. 127 (2), 163–182.

Liao, X., Sharma, N., Kapadia, F., Zhou, G., Lu, Y., Hong, H., Paruchuri, K., Mahabeleshwar, G.H., Dalmas, E., Venteclef, N., et al., 2011. Krüppel-like factor 4 regulates macrophage polarization. J. Clin. Invest. 121 (7), 2736.

Lim, Y.-P., Peng, C.-Y., Liao, W.-L., Hung, D.-Z., Tien, N., Chen, C.-Y., Chang, S.-Y., Chang, C.-Y., Tsai, F.-J., Wan, L., 2013. Genetic variation in nos2a is associated with a sustained virological response to peginterferon plus ribavirin therapy for chronic hepatitis c in taiwanese chinese. J. Med. Virol. 85 (7), 1206–1214.

Lyashchenko, K.P., Greenwald, R., Esfandiari, J., Greenwald, D., Nacy, C.A., Gibson, S., Didier, P.J., Washington, M., Szczerba, P., Motzel, S., et al., 2007. Primatb stat-pak assay, a novel, rapid lateral-flow test for tuberculosis in nonhuman primates. Clin. Vaccine Immunol. 14 (9), 1158–1164.

MacMicking, J., Xie, Q.-w., Nathan, C., 1997. Nitric oxide and macrophage function. Annu. Rev. Immunol. 15 (1), 323–350.

McAuliffe, J., Vogel, L., Roberts, A., Fahle, G., Fischer, S., Shieh, W.-J., Butler, E., Zaki, S., St Claire, M., Murphy, B., et al., 2004. Replication of sars coronavirus administered into the respiratory tract of african green, rhesus and cynomolgus monkeys. Virology 330 (1), 8–15.

Meyer, D., Zeileis, A., Hornik, K., 2006. vcd: Visualizing categorical data, R package version, 1-0.

Mgbemena, V., Segovia, J.A., Chang, T.-H., Tsai, S.-Y., Cole, G.T., Hung, C.-Y., Bose, S., 2012. Transactivation of inducible nitric oxide synthase gene by kruppel-like factor 6 regulates apoptosis during influenza a virus infection. J. Immunol. 189 (2), 606–615.

Mgbemena, V., Segovia, J., Chang, T.-H., Bose, S., 2013. Klf6 and inos regulates apoptosis during respiratory syncytial virus infection. Cell. Immunol. 283 (1), 1–7.

Nanashima, K., Mawatari, T., Tahara, N., Higuchi, N., Nakaura, A., Inamine, T., Kondo, S., Yanagihara, K., Fukushima, K., Suyama, N., et al., 2012. Genetic variants in antioxidant pathway: risk factors for hepatotoxicity in tuberculosis patients. Tuberculosis 92 (3), 253–259.

Nunokawa, Y., Ishida, N., Tanaka, S., 1994. Promoter analysis of human inducible nitric oxide synthase gene associated with cardiovascular homeostasis. Biochem. Biophys. Res. Commun. 200 (2), 802–807, doi:http://dx.doi.org/10.1006/bbrc.1994.1522. URL http://www.sciencedirect.com/science/article/pii/S0006291X84715221.

Obermajer, N., Wong, J.L., Edwards, R.P., Chen, K., Scott, M., Khader, S., Kolls, J.K., Odunsi, K., Billiar, T.R., Kalinski, P., 2013. Induction and stability of human th17 cells require endogenous nos2 and cgmp-dependent no signaling. J. Exp. Med. 210 (7), 1433–1445.

Ohmori, Y., Hamilton, T.A., 2001. Requirement for stat1 in lps-induced gene expression in macrophages. J. Leukoc. Biol. 69 (4), 598–604.

Oussaief, L., Ramírez, V., Hippocrate, A., Arbach, H., Cochet, C., Proust, A., Raphaël, M., Khelifa, R., Joab, I., 2011. Nf-κb-mediated modulation of inducible nitric oxide synthase activity controls induction of the epstein-barr virus productive cycle by transforming growth factor beta 1. J. Virol. 85 (13), 6502–6512.

Paradis, E., Claude, J., Strimmer, K., 2004. APE: analyses of phylogenetics and evolution in R language. Bioinformatics 20, 289–290.

Park, J.M., Baeg, M.-K., Lim, C.-H., Cho, Y.K., Choi, M.-G., 2014. Nitric oxide synthase gene polymorphisms in functional dyspepsia. Dig. Dis. Sci. 59 (1), 72–77.

Pautz, A., Art, J., Hahn, S., Nowag, S., Voss, C., Kleinert, H., 2010. Regulation of the expression of inducible nitric oxide synthase. Nitric Oxide 23 (2), 75–93.

Planche, T., Macallan, D.C., Sobande, T., Borrmann, S., Kun, J.F., Krishna, S., Kremsner, P.G., 2010. Nitric oxide generation in children with malaria and the nos2g-954c promoter polymorphism. Am. J. Physiol. Regul. Integr. Comp. Physiol. 299 (5), R1248–R1253.

Quandt, K., Frech, K., Karas, H., Wingender, E., Werner, T., 1995. Matlnd and matlnspector: new fast and versatile tools for detection of consensus matches in nucleotide sequence data. Nucleic Acids Res. 23 (23), 4878–4884.

Rafiei, A., Hosseini, V., Janbabai, G., Fazli, B., Ajami, A., Hosseini-Khah, Z., Gilbreath, J., Merrell, D.S., 2012. Inducible nitric oxide synthetase genotype and helicobacter pylori infection affect gastric cancer risk. World J. Gastroenterol. 18 (35), 4917.

R Core Team, 2014. R: A Language and Environment for Statistical Computing, R Foundation for Statistical Computing, Vienna, Austria. URL http://www.R-project.org.

Roodgar, M., Lackner, A., Kaushal, D., Sankaran, S., Dandekar, S., Satkoski Trask, J., Drake, C., Smith, D.G., 2013. Expression levels of 10 candidate genes in lung tissue of vaccinated and tb-infected cynomolgus macaques. J. Med. Primatol. 42 (3), 161–164.

Samardzic, T., Jankovic, V., Stosic-Grujicic, S., Trajkovic, V., 2001. Stat1 is required for inos activation, but not il-6 production in murine fibroblasts. Cytokine 13 (3), 179–182.

Stan Development Team, 2013. Stan: A c++ library for probability and sampling, version 2.0. URL http://mc-stan.org/.

Stan Development Team, 2014. Stan Modeling Language Users Guide and Reference Manual, Version 2.2. URL http://mc-stan.org/.

Tang, R.S., MacPhail, M., Schickli, J.H., Kaur, J., Robinson, C.L., Lawlor, H.A., Guzzetta, J.M., Spaete, R.R., Haller, A.A., 2004. Parainfluenza virus type 3 expressing the native or soluble fusion (f) protein of respiratory syncytial virus (rsv) confers protection from rsv infection in african green monkeys. J. Virol. 78 (20), 11198–11207.

Tibshirani, R., 1996. Regression shrinkage and selection via the lasso. J. R. Stat. Soc. Ser. B, 267–288.

Tosi, A.J., Morales, J.C., Melnick, D.J., 2000. Comparison of y chromosome and mtdna phylogenies leads to unique inferences of macaque evolutionary history. Mol. Phylogenet. Evol. 17 (2), 133–144.

Uffort, D.G., Grimm, E.A., Ellerhorst, J.A., 2009. Nf-κb mediates mitogen-activated protein kinase pathway-dependent inos expression in human melanoma. J. Invest. Dermatol. 129 (1), 148–154.

Wang, Z., Feng, K., Yue, M., Lu, X., Zheng, Q., Zhang, H., Zhai, Y., Li, P., Yu, L., Cai, M., et al., 2013. A non-synonymous snp in the nos2 associated with septic shock in patients with sepsis in chinese populations. Hum. Genet. 132 (3), 337–346.

Warke, V.G., Nambiar, M.P., Krishnan, S., Tenbrock, K., Geller, D.A., Koritschoner, N.P., Atkins, J.L., Farber, D.L., Tsokos, G.C., 2003. Transcriptional activation of the human inducible nitric-oxide synthase promoter by krüppel-like factor 6. J. Biol. Chem. 278 (17), 14812–14819.

Waterhouse, A.M., Procter, J.B., Martin, D.M., Clamp, M., Barton, G.J., 2009. Jalview version 2a multiple sequence alignment editor and analysis workbench. Bioinformatics 25 (9), 1189–1191.

Wienerroither, S., Rauch, I., Rosebrock, F., Jamieson, A.M., Bradner, J., Muhar, M., Zuber, J., Müller, M., Decker, T., 2014. Regulation of no synthesis, local inflammation, and innate immunity to pathogens by bet family proteins. Mol. Cell. Biol. 34 (3), 415–427.

Zhang, Y., Li, C., Li, K., Liu, L., Jian, Z., Gao, T., 2011. Analysis of inducible nitric oxide synthase gene polymorphisms in vitiligo in han chinese people. PloS One 6 (12), e27077.

Zhao, W., Cha, E.N., Lee, C., Park, C.Y., Schindler, C., 2007. Stat2-dependent regulation of mhc class ii expression. J. Immunol. 179 (1), 463–471.

UNCORRECTED PROOF

Please cite this article in press as: Roodgar, M., et al. Inducible nitric oxide synthase (*iNOS*) regulatory region variation in non-human primates. Infect. Genet. Evol. (2015), http://dx.doi.org/10.1016/j.meegid.2015.01.015